Editorial

Huajun Zeng, Yuduo Ming, Tao Jiang, and Cheng Jin*

Exact solutions of a class of generalized nanofluidic models

https://doi.org/10.1515/phys-2024-0068
received December 13, 2023; accepted July 22, 2024

Abstract: Nanofluid, a significant branch of fluid mechanics, plays a pivotal role in thermal management, optics, biomedical engineering, energy harvesting, and other fields. The nanoparticles present in the fluid render the continuum mechanics ineffective, necessitating the adoption of fractional calculus to elucidate the effects of nanoparticles on the motion properties of the nanofluid. This article applies the modified extended tanh-function technique to solve two classical Schrödinger equations, the fractional Phi-4 model and the conformable fractional Boussinesq model, for nanofluids. Multiple exact solutions are obtained, and the corresponding graphical representations are provided to elucidate the basic properties of the nanofluid. This article provides new research perspectives for the development of nanofluids.

Keywords: nanofluid, the fractional Phi-4 model, the conformable fractional Boussinesq model, modified extended tanh-function technique, exact solution

1 Introduction

Nanofluid is a composite fluid system in which nanoparticles are dispersed in a base fluid [1,2]. The addition of nanoparticles can alter the properties and behavior of the base fluid, thereby imparting unique characteristics to the nanofluid. The effects of nanofluids can be demonstrated in a variety of ways. First, nanofluids can enhance the thermal conductivity of the base fluid, resulting in a higher thermal conductivity [3,4]. This enables the widespread applications of nanofluids in the field of thermal management, such as radiator [5], and energy harvesting [6,7], which is distinct from the traditional spring-pendulum system [8,9]. Second, nanofluids play a significant role in the field of optics, as they can be used to fabricate materials with special optical properties, such as transparent conductive films [10] and optical sensors [11]. Moreover, nanofluids are utilized in the biomedical field for the advancement of nanodrug delivery systems [12], biosensors [13], and blood flow [14], among other applications.

In fact, nanofluid can be considered a branch of fluid mechanics, which is a discipline within the broader field of physics that studies the motion and behavior of liquids and gases. It encompasses aspects such as fluid dynamics, statics, and heat and mass transfer. In contrast, nanofluid research is focused on the dispersion effects of nanoparticles in the base fluid at the nanoscale and their influence on the macroscopic properties of the fluid. The study of nanofluids necessitates the consideration of factors pertaining to the nanoscale, including surface forces, charge effects, and the wetting behavior of nanoparticles. Kou *et al.* demonstrated that the remarkable phenomena observed in nanofluids can be explained by the fractal boundary-layer theory [15]. A fractal boundary layer can result in minimal friction between the fractal boundary and the flowing fluid, as observed in the case of waving dunes [16,17]. It is, however, important to note that there is a certain connection between nanofluids and traditional fluid mechanics. The foundation of nanofluid research remains firmly rooted in the theoretical and experimental frameworks of traditional fluid mechanics. The behavior of nanofluids can typically be explained and predicted using principles and models of fluid mechanics [18]. Concurrently, the investigation of nanofluids offers a novel avenue for research in fluid mechanics, facilitating enhanced comprehension and exploitation of fluid dynamics. Consequently, there exists a close connection and interdependency between nanofluids and traditional fluid mechanics.

In recent years, fractal thermodynamics [19,20] has emerged as a promising approach to address challenges in fluid mechanics that conventional fluid mechanics has been unable to resolve. Fractional partial differential

*** Corresponding author: Cheng Jin,** School of Statistics and Mathematics, Zhejiang Gongshang University, Hangzhou, 310018, China, e-mail: 1936283207@qq.com
Huajun Zeng: School of Statistics and Mathematics, Zhejiang Gongshang University, Hangzhou, 310018, China
Yuduo Ming: School of Optoelectronic Engineering, Changchun University of Science and Technology, Changchun, 130013, China
Tao Jiang: Hangzhou College of Commerce, Zhejiang Gongshang University, Hangzhou, 311599, China

equations (FPDEs) have also gained significant traction in various applications. FPDEs represent an extension of traditional integer-order partial differential equations, wherein the derivatives assume a fractional-order form. The most commonly employed fractional-order derivatives include the Caputo fractional derivative [21,22], the Caputo–Fabrizio fractional derivative [23,24], and the Jumarie-modified Riemann–Liouville fractional derivative [25]. The application of FPDEs in fluid mechanics encompasses a multitude of facets. First, they are employed to describe the transport behavior of fluids in non-local media. For instance, in the context of non-local diffusion problems, fractional diffusion equations are more effective at describing diffusion phenomena [26]. Second, FPDEs can be employed to describe non-local diffusion phenomena with long-tail distributions [27] and other similar phenomena. In conclusion, FPDEs have made a substantial impact on the advancement of fluid mechanics. They provide a mathematical framework for more accurately describing non-local and non-linear phenomena. The introduction of fractional derivatives enables the characterization of the transport behavior and dynamic characteristics of fluids in complex media. Moreover, the utilization of FPDEs facilitates a more comprehensive and accurate modeling of fluid motion. These applications not only facilitate a more profound comprehension of fluid behavior but also furnish novel mathematical instruments and methodologies for the resolution of practical engineering issues and the formulation of corresponding control strategies.

Consequently, this study aims to identify precise solutions for selected classical fluid particle dynamics equations in fluid mechanics. The objective is to contribute to the development of nanofluids. Specifically, this study selects two Schrödinger equations for investigation: the fractional Phi-4 model and the conformable fractional Boussinesq model. The application of Schrödinger equations in fluid mechanics provides a quantum mechanical framework for the study of wave–particle duality, quantum transport, and the interactions of particles in fluid media [28]. This approach to quantum fluid mechanics enhances our comprehension of fluid phenomena and illuminates the pivotal role of quantum effects in fluid dynamics. The solutions of the nonlinear Schrödinger equation can be obtained through a variety of methods, including the $(\frac{G'}{G})$-expansion method [29], the extended tanh-function method [30], the extended rational sin–cos and sinh–cosh methods [31], the new extended direct algebraic method [32], and the exp-function method [33]. In this article, we will employ the modified extended tanh-function technique of fractional complex transformation to identify exact solutions to the subsequent two models:

1) the fractional Phi-4 model [34,35]:

$$D_t^{2\alpha}u - D_x^{2\alpha}u + a^2u + bu^3 = 0, \tag{1}$$

where a and b are the real constants and $0 < \alpha, \beta < 1$. The Klein–Gordon equation, a fundamental Schrödinger equation, has found application in a number of fields, including optics, thermal science, nanofluids, and nonlinear vibration. The Phi-4 model represents a specific shape within this equation and has been widely used for modeling purposes. In recent times, researchers have employed a variety of methodologies to investigate the fractional Phi-4 model. For instance, in their work [36], new exact analytical solutions for the time-fractional Phi-4 model were presented using an extended direct algebraic method. Körpinar employed a variety of mapping techniques utilizing the conformal fractional derivative operator to address the aforementioned issue [37]. The construction of new exact solutions for the time-fractional Phi-4 model was achieved by applying the $(\frac{G'}{G}, \frac{1}{G})$ expansion technique, as detailed in the study by Hwang *et al.* [3]. In the study by Akram *et al.* [35], the traveling wave solutions for the space–time fractional Phi-4 model were constructed using the extended $(\frac{G'}{G^2})$ evolution method and the modified auxiliary equation method. In their investigation of computational wave solutions of Eq. (1), Khater employed the novel Kudryashov schemes, as described in the study by Khater [38].

2) The conformable fractional Boussinesq model [39]:

$$D_t^{2\alpha}u + D_x^{2\beta}u + D_x^{2\beta}(u^2) + D_x^{4\beta}u = 0, \tag{2}$$

where $0 < \alpha, \beta < 1$. The Schrödinger–Boussinesq equation, a classic equation in fluid mechanics, occupies a prominent position in the field. Subsequently, the equation was extended by introducing fractional derivatives, leading to extensive applications in various fields. In particular, the fractional Boussinesq equation is employed extensively to model the propagation grid and the nonlinear chain of small-amplitude nonlinear long waves on the water surface. These models have a wide range of engineering applications, including diffraction, shallow water predictions, refraction, and harmonic interactions [40]. A number of methods have been developed to solve this equation in an effective manner. For instance, in their study by Hosseini and Ansari [41], the validated modified Kudryashov method was employed to identify exact solutions to this equation. In order to identify exact solutions for the fractional Boussinesq model [42], the simply improved $\tan(\frac{\phi(\xi)}{2})$ method was employed. The study of exact solutions for the new generalized perturbed form of this equation was carried out by Nisar *et al.* [43], who employed the modified Kudryashov method and the improved generalized Riccati equation mapping method. Moreover, Chen

et al. employed the $(\frac{G'}{G^2})$-expansion method and the unified F-expansion method to identify exact wave solutions to this equation [39].

The following section outlines the structure of this article. Section 2 provides a comprehensive introduction to the solution method. Subsequently, Sections 3 and 4 address the fractional Phi-4 model and the conformal fractional Boussinesq model, respectively. Finally, the conclusions are presented in Section 5.

2 Methodology

Considering the FPDE

$$P(u, D_t^\alpha u, D_x^\beta u, D_t^\alpha D_t^\alpha u, D_t^\alpha D_x^\beta u, D_x^\beta D_x^\beta u, \ldots) = 0, \quad (0 < \alpha, \beta < 1), \tag{3}$$

where $D_t^\alpha u, D_x^\beta u, D_t^\alpha D_t^\alpha u, \ldots$ are the notations of the fractional derivative. The polynomial P is formulated in terms of the variable u and its corresponding partial derivatives. In this article, we adopt the fractional derivative in the modified Riemann–Liouville sense [25]. Some properties of the proposed derivative are described in the study by Jumarie [44] listed as follows:

$$D_t^\alpha t^r = \frac{\Gamma(1 + r)}{\Gamma(1 + r - \alpha)} t^{r-\alpha}, \tag{4}$$

$$D_t^\alpha (cf(x)) = cD_t^\alpha f(x), \quad c \text{ is a constant}, \tag{5}$$

$$D_t^\alpha (f(w) + g(w)) = D_t^\alpha f(w) + D_t^\alpha g(w). \tag{6}$$

In this article, as for fractional calculus, we used the following chain rule [45]:

$$\begin{aligned} D_t^\alpha u &= \sigma_t \frac{\partial u(\xi)}{\mathrm{d}\xi} D_t^\alpha \xi, \\ D_x^\alpha u &= \sigma_x \frac{\partial u(\xi)}{\mathrm{d}\xi} D_x^\alpha \xi, \\ D_t^{2\alpha} u &= (\sigma_t)^2 \frac{\partial^2 u(\xi)}{\mathrm{d}\xi^2} D_t^{2\alpha} \xi, \\ D_x^{2\alpha} u &= (\sigma_x)^2 \frac{\partial^2 u(\xi)}{\mathrm{d}\xi^2} D_x^{2\alpha} \xi, \end{aligned} \tag{7}$$

where σ_t and σ_x are the sigma indices. We take $\sigma_t = \sigma_x = L$ (L is a constant), without loss of generality.

Based on the aforementioned preliminaries, the general steps to solve Eqs (1) and (2) using the modified extended tanh-function technique are as follows:

Step 1: Using the nonlinear fractional complex wave transformation [45,46]:

$$\begin{aligned} u(x, t) &= u(\xi), \\ \xi &= \frac{lx^\beta}{\Gamma(\beta + 1)} + \frac{kt^\alpha}{\Gamma(\alpha + 1)}, \end{aligned} \tag{8}$$

where l and k are the constants and $l, k \neq 0$. Eq. (8) is the famous fractional complex transform [47,48].

Substituting Eqs (7) and (8) into Eq. (3), we have

$$Q(u, u', u'', \ldots) = 0, \tag{9}$$

where $u' = \frac{\mathrm{d}u}{\mathrm{d}\xi}$, $u'' = \frac{\mathrm{d}^2 u}{\mathrm{d}\xi^2} \cdots$, Q present the polynomial function that contains u and the derivatives of u with respect to ξ.

Step 2: Expressing the solution of ordinary differential Eq. (9) as a polynomial form of ψ:

$$u(\xi) = \sum_{i=0}^{n} a_i \psi^i(\xi), \tag{10}$$

where $\psi = \psi(\xi)$ conforming to the following Riccati equation:

$$\psi' = \varepsilon + \psi^2, \tag{11}$$

where ε is an arbitrary constant and $a_i (i = 0, 1, 2, \ldots, n)$ are the indefinite constants. And by equating the highest order of the nonlinear term with that of the derivative term, the value of the positive integer n can be found. For ψ, the following three types of solutions are determined according to different values of the constant ε:

$$\begin{cases} \psi = -\sqrt{-\varepsilon} \tanh \sqrt{-\varepsilon}\, \xi, & \varepsilon < 0, \\ \psi = -\sqrt{-\varepsilon} \coth \sqrt{-\varepsilon}\, \xi, & \varepsilon < 0, \\ \psi = \sqrt{\varepsilon} \tan \sqrt{\varepsilon}\, \xi, & \varepsilon > 0, \\ \psi = \sqrt{\varepsilon} \cot \sqrt{\varepsilon}\, \xi, & \varepsilon > 0, \\ \psi = -\dfrac{1}{\xi}, & \varepsilon = 0. \end{cases} \tag{12}$$

Step 3: Substituting Eq. (10) into Eq. (9), using Eq. (11) to iterate and combining the terms of ε, which has the same power, setting the coefficients and constant terms of each power to zero. Then, we obtain the over-determined algebraic equations about l, k, L, ε and a_i $(i = 0, 1, 2, \ldots, n)$. Finally, we acquire multiply different types of exact solutions about Eq. (3) by calculating the parameters and substituting into Eq. (10).

3 Exact solution of the fractional Phi-4 model

Employing the subsequent traveling wave transformation:

$$u(x,t) = u(\xi),$$
$$\xi = \frac{lx^{\alpha}}{\Gamma(\alpha+1)} + \frac{kt^{\alpha}}{\Gamma(\alpha+1)}, \tag{13}$$

the original Eq. (1) is transformed into a nonlinear ordinary differential equation:

$$L^2k^2u'' - L^2l^2u'' + a^2u + bu^3 = 0, \tag{14}$$

balancing term "u^3," which is the highest order derivative and the nonlinear term "u''," we obtain $n = 1$. Thus, Eq. (10) becomes

$$u(\xi) = a_0 + a_1\psi(\xi). \tag{15}$$

If we substitute Eqs (11) and (15) into Eq. (14) and then combine the same power terms of ψ and set its coefficient to zero, we obtain the nonlinear algebraic overdetermined systems around a_0, a_1, a, b, l, k, L, and ε:

$$\begin{aligned} &a_0(a^2 + a_0b) = 0,\\ &a^2 + 3(a_0)^2b + 2(k^2 - l^2)L^2\varepsilon = 0,\\ &3a_0(a_1)^2b = 0,\\ &(a_1)^3b + 2a_1(k^2 - l^2)L^2 = 0. \end{aligned} \tag{16}$$

Solving the aforementioned set of equations using Mathematica, the results can be obtained:

Case 1.

$$a_0 = 0, \quad a_1 = -\frac{\sqrt{2}\sqrt{-k^2L^2 + l^2L^2}}{\sqrt{b}}, \quad \varepsilon = -\frac{a^2}{2(k^2 - l^2)L^2}.$$

According to the solution, in order for the original equation to have an accurate solution of real numbers, there must be $|l| > |k|$ and $l, k \neq 0$. Therefore, in Case 1, according to the different values of ε, we have

(I) When $a = 0, \varepsilon = 0$, which produce

$$u_1(\xi) = L\sqrt{\frac{2(l^2 - k^2)}{b}}\frac{1}{\xi}, \quad \varepsilon = 0, \tag{17}$$

where $\xi = \frac{lx^{\alpha}}{\Gamma(\alpha+1)} + \frac{kt^{\alpha}}{\Gamma(\alpha+1)}$, l, k are the arbitrary constants and $|l| > |k| \neq 0$.

The numerical simulation image of $u_1(\xi)$ is shown in Figure 1.

(II) When $a \neq 0, \varepsilon > 0$, which produce

$$u_2(\xi) = -\frac{a}{\sqrt{b}}\tan\frac{a}{L\sqrt{2(l^2 - k^2)}}\xi, \quad \varepsilon > 0, \tag{18}$$

$$u_3(\xi) = -\frac{a}{\sqrt{b}}\cot\frac{a}{L\sqrt{2(l^2 - k^2)}}\xi, \quad \varepsilon > 0, \tag{19}$$

where $\xi = \frac{lx^{\alpha}}{\Gamma(\alpha+1)} + \frac{kt^{\alpha}}{\Gamma(\alpha+1)}$, l, k are the arbitrary constants and $|l| > |k| \neq 0$.

The numerical simulation images of $u_2(\xi)$ and $u_3(\xi)$ are shown in Figure 2.

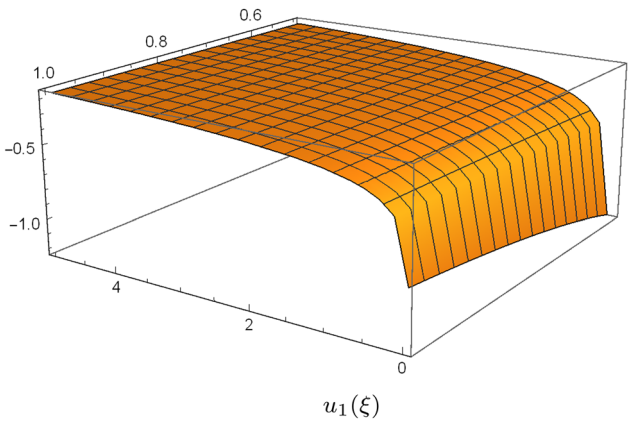

Figure 1: Three-dimensional plot of $u_1(\xi)$ in Case 1 for $\alpha = \frac{1}{2}$, $a = 0$, $b = k = L = 1$, and $l = 2$.

Case 2.

$$a_0 = 0, \quad a_1 = \frac{\sqrt{2}\sqrt{-k^2L^2 + l^2L^2}}{\sqrt{b}}, \quad \varepsilon = -\frac{a^2}{2(k^2 - l^2)L^2}.$$

Similarly, there must be $|l| > |k|$ and $l, k \neq 0$. Therefore, in Case 2, according to the different values of ε, we have

(I) When $a = 0, \varepsilon = 0$, which produce

$$u_4(\xi) = -L\sqrt{\frac{2(l^2 - k^2)}{b}}\frac{1}{\xi}, \quad \varepsilon = 0, \tag{20}$$

where $\xi = \frac{lx^{\alpha}}{\Gamma(\alpha+1)} + \frac{kt^{\alpha}}{\Gamma(\alpha+1)}$, l, k are the arbitrary constants and $|l| > |k| \neq 0$.

The numerical simulation image of $u_4(\xi)$ is shown in Figure 3.

(II) When $a \neq 0, \varepsilon > 0$, which produce

$$u_5(\xi) = \frac{a}{\sqrt{b}}\tan\frac{a}{L\sqrt{2(l^2 - k^2)}}\xi, \quad \varepsilon > 0, \tag{21}$$

$$u_6(\xi) = \frac{a}{\sqrt{b}}\cot\frac{a}{L\sqrt{2(l^2 - k^2)}}\xi, \quad \varepsilon > 0, \tag{22}$$

where $\xi = \frac{lx^{\alpha}}{\Gamma(\alpha+1)} + \frac{kt^{\alpha}}{\Gamma(\alpha+1)}$, l, k are the arbitrary constants and $|l| > |k| \neq 0$.

The numerical simulation images of $u_5(\xi)$ and $u_6(\xi)$ are shown in Figure 4.

4 Exact solution of the conformable fractional Boussinesq model

Supposing that $u(x,t) = u(\xi)$, where ξ is given by Eq. (8). Then, Eq. (2) can be turned into the following equation of ordinary differential equations (ODEs):

$$L^2k^2u'' + L^2l^2u'' + L^2l^2(u^2)'' + L^4l^4u^{(4)} = 0. \tag{23}$$

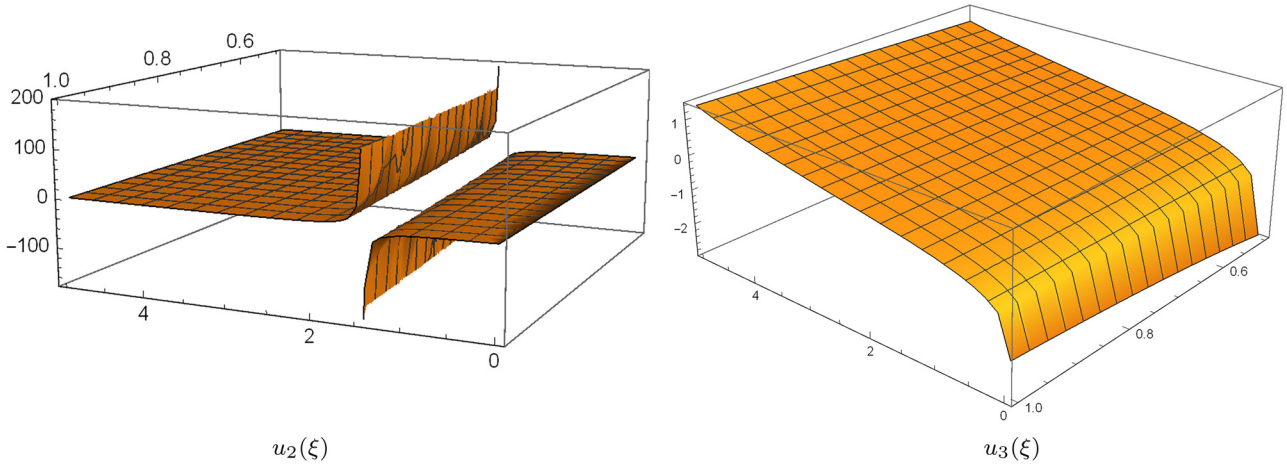

$u_2(\xi)$ $u_3(\xi)$

Figure 2: Three-dimensional plots of $u_2(\xi)$ and $u_3(\xi)$ in Case 1 for $\alpha = \frac{1}{2}$, $a = b = k = L = 1$, and $l = 2$.

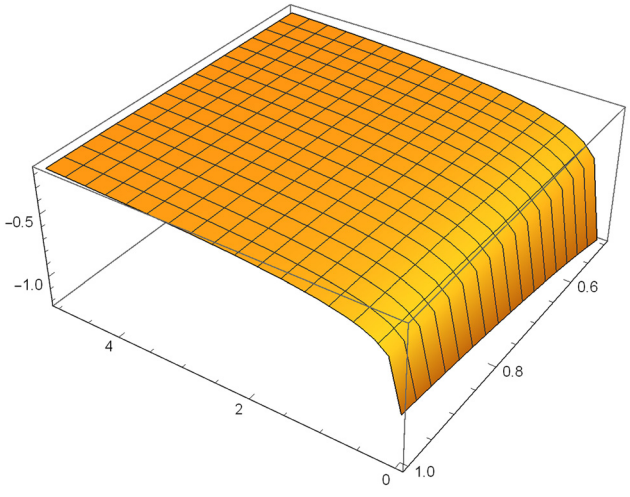

$u_4(\xi)$

Figure 3: Three-dimensional plot of $u_4(\xi)$ in Case 1 for $\alpha = \frac{1}{2}$, $a = 0$, $b = k = L = 1$, and $l = 2$.

Integrating twice and the integral constant is equal to zero, Eq. (23) turns into

$$k^2u + l^2u + l^2u^2 + L^2l^4u'' = 0. \tag{24}$$

This equation with a quadratic nonlinearity has some amazing properties as discussed in the study by He and Liu [49]. Balancing the term "u^2" and the term "u''," we obtain $n = 2$. Thus, Eq. (10) becomes

$$u(\xi) = a_0 + a_1\psi(\xi) + a_2\psi^2(\xi). \tag{25}$$

Substitute Eqs (11) and (25) into Eq. (24), and collect all terms with the same power of ψ. Equating each coefficient to zero yields the following set of algebraic equations for a_0, a_1, a_2, l, k, L, and ε:

$$\begin{aligned}
&a_0^2l^2 + a_0(k^2 + l^2) + 2a_2l^4L^2\varepsilon^2 = 0,\\
&a_1(k^2 + l^2(1 + 2a_0 + 2l^2L^2\varepsilon)) = 0,\\
&a_1^2l^2 + a_2(k^2 + l^2 + 2a_0l^2 + 8l^4L^2\varepsilon) = 0,\\
&a_1l^2(a_2 + l^2L^2) = 0,\\
&a_2 + 6l^2L^2 = 0.
\end{aligned} \tag{26}$$

Solving the aforementioned algebraic equations, we obtain:

Case 1.

$$a_0 = \frac{k^2 + l^2}{2l^2}, \quad a_1 = 0, \quad a_2 = -6l^2L^2, \quad \varepsilon = -\frac{k^2 + l^2}{4l^4L^2} < 0,$$

which produces

$$u_1(\xi) = \frac{k^2 + l^2}{2l^2} - \frac{3(k^2 + l^2)}{2l^2}\tanh^2\frac{\sqrt{k^2 + l^2}}{2l^2L}\xi, \quad \varepsilon < 0, \tag{27}$$

$$u_2(\xi) = \frac{k^2 + l^2}{2l^2} - \frac{3(k^2 + l^2)}{2l^2}\coth^2\frac{\sqrt{k^2 + l^2}}{2l^2L}\xi, \quad \varepsilon < 0, \tag{28}$$

where $\xi = \frac{lx^\beta}{\Gamma(\beta+1)} + \frac{kt^\alpha}{\Gamma(\alpha+1)}$, l, k are the arbitrary constants and $l, k \neq 0$.

For more convenience, the graphical representations of Eq. (27) and Eq. (28) are shown in Figure 5.

Case 2.

$$a_0 = -\frac{3(k^2 + l^2)}{2l^2}, \quad a_1 = 0, \quad a_2 = -6l^2L^2, \quad \varepsilon = \frac{k^2 + l^2}{4l^4L^2} > 0,$$

which produces

$$u_3(\xi) = -\frac{3(k^2 + l^2)}{2l^2}\sec^2\frac{\sqrt{k^2 + l^2}}{2l^2L}\xi, \quad \varepsilon > 0, \tag{29}$$

$$u_4(\xi) = -\frac{3(k^2 + l^2)}{2l^2}\csc^2\frac{\sqrt{k^2 + l^2}}{2l^2L}\xi, \quad \varepsilon > 0, \tag{30}$$

where $\xi = \frac{lx^\beta}{\Gamma(\beta+1)} + \frac{kt^\alpha}{\Gamma(\alpha+1)}$, l, k are the arbitrary constants and $l, k \neq 0$.

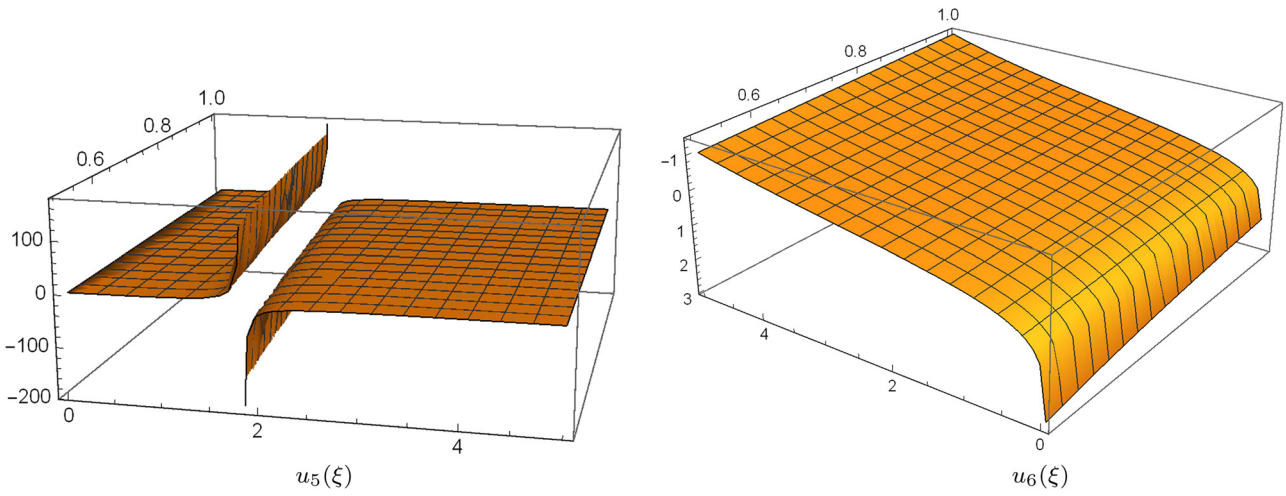

Figure 4: Three-dimensional plots of $u_5(\xi)$ and $u_6(\xi)$ in Case 1 for $\alpha = \frac{1}{2}$, $a = b = k = L = 1$, and $l = 2$.

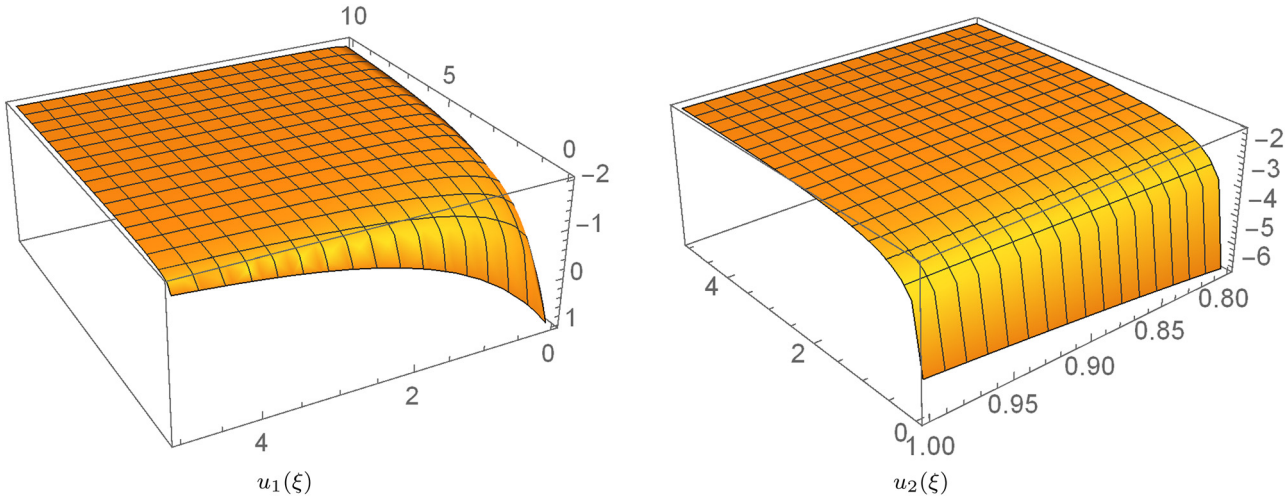

Figure 5: Three-dimensional plots of $u_1(\xi)$ and $u_2(\xi)$ in Case 1 of Eq. (2), with $\alpha = \beta = \frac{1}{2}$, $l = k = L = 1$.

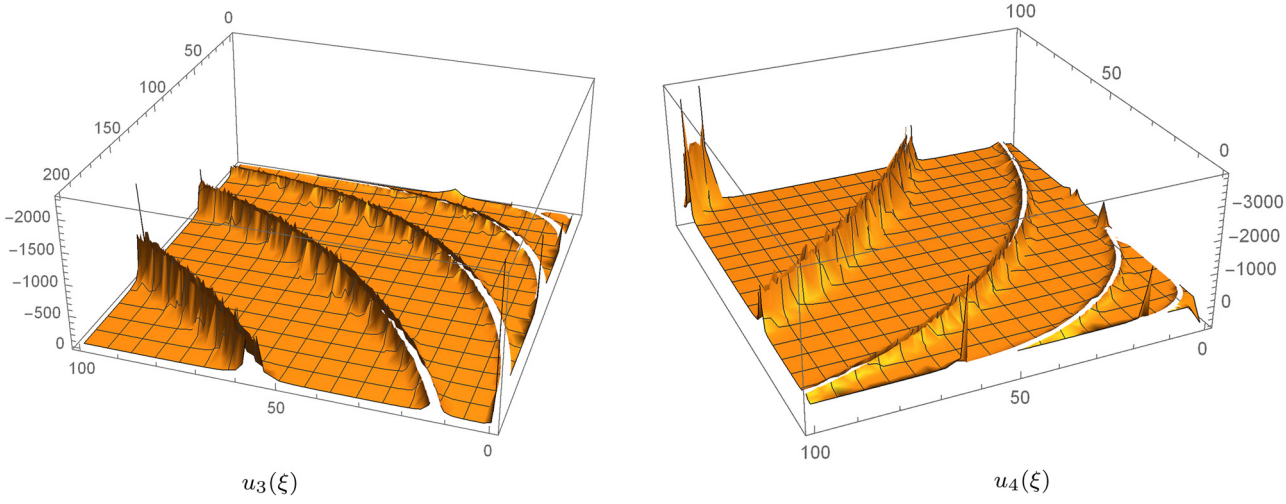

Figure 6: Three-dimensional plots of $u_3(\xi)$ and $u_4(\xi)$ in Case 2 of Eq. (2), with $\alpha = \beta = \frac{1}{2}$, $l = k = L = 1$.

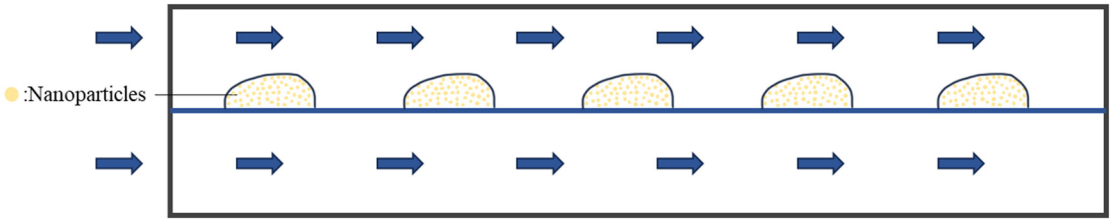

Figure 7: Nanofluid in a micro-channel.

The graphical representations of Eqs (29) and (30) are shown in Figure 6, respectively.

5 Discussion and conclusion

As illustrated earlier, the dynamical properties of nanofluids can be controlled by the fractional order. Nanofluids have been successfully applied to fractal pattern dynamic [50], fractal financial system [51], and MEMS systems [52], where the nanoparticles or nanoparticle-induced boundaries play an important role in the systems' efficiency and reliability. For instance, when a nanofluid flows through a nano/micro-device as shown in Figure 7, it can significantly enhance the thermal conduction, thereby enabling the temperature to be maintained below an unsafe threshold.

As shown earlier, the dynamical properties of a nanofluid are a function of t^{α} and x^{β}, rather than t and x. The values of α and β can be determined by the He–Liu fractal dimension formulation [53], which allows for the reflection of the nanoparticles' size and distribution. This is not possible in traditional fluid mechanics, and it can save a significant amount of time during theoretical analysis compared to the multi-scale numerical approach to the two-phase fluid [54].

This article focuses on nanofluids and applies the modified extended Tanh function technique to solve two classical fractional Schrödinger equations in fluid mechanics: the Phi-4 fractional model and the conformal fractional Boussinesq model. The exact solutions of these two equations are presented graphically. These solutions have direct practical applications in the field of nanofluids. We posit that this article offers numerous opportunities to advance the development of nanofluids and can serve as a good example for future research.

Funding information: This research was supported by the National Natural Science Foundation of China (11971433), First Class Discipline of Zhejiang-A (Zhejiang Gongshang University-Statistics), the Characteristic & Preponderant Discipline of Key Construction Universities in Zhejiang Province (Zhejiang Gongshang University-Statistics), Collaborative Innovation Center of Statistical Data Engineering Technology and Application.

Author contributions: All authors have accepted responsibility for the entire content of this manuscript and approved its submission.

Conflict of interest: The authors state no conflict of interest.

References

[1] He JH, Elgazery NS, Elagamy K, Abd-Elazem NY. Efficacy of a modulated viscosity-dependent temperature/nanoparticles concentration parameter on a nonlinear radiative electromagneto-nanofluid flow along an elongated stretching sheet. J Appl Comput Mech. 2023;9(3):848–60.

[2] Kumar K, Chauhan PR, Kumar R, Bharj RS. Irreversibility analysis in Al2O3-water nanofluid flow with variable property. Facta Univ-Ser Mech. 2022;20(3):503–18.

[3] Hwang YJ, Ahn YC, Shin HS, Lee CG, Kim GT, Park HS, et al. Investigation on characteristics of thermal conductivity enhancement of nanofluids. Curr Appl Phys. 2006;6(6):1068–71.

[4] Asshaari I, Jedi A, Abdullah S. Brownian motion and thermophoresis effects in co-flowing carbon nanotubes towards a moving plate. Results Phys. 2023;44:106165.

[5] Bhogare RA, Kothawale BS. Performance investigation of automobile radiator operated with Al2O3 based nanofluid. J Mech Civ Eng. 2014;11(3):23–30.

[6] He JH, Abd-Elazem NY. The carbon nanotube-embedded boundary layer theory for energy harvesting. Facta Univ-Ser Mech. 2022;20(2):211–35.

[7] Wang QL, He JH, Liu Z. Intelligent nanomaterials for solar energy harvesting: from polar bear hairs to unsmooth nanofiber fabrication. Front Bioeng Biotech. 2022;10:926253.

[8] He CH, Amer TS, Tian D, Abolila AF, Galal AA. Controlling the kinematics of a spring-pendulum system using an energy harvesting device. J Low Freq Noise V A. 2022;41(3):1234–57.

[9] He CH, El-Dib YO. A heuristic review on the homotopy perturbation method for non-conservative oscillators. J Low Freq Noise V A. 2022;41(2):572–603.

[10] Ilatovskii DA, Gilshtein EP, Glukhova OE, Nasibulin AG. Transparent conducting films based on carbon nanotubes: rational design toward the theoretical limit. Adv Sci. 2022;9(24):2201673.
[11] Hu XY, Abbasi R, Wachsmann-Hogiu S. Microfluidics on lensless, semiconductor optical image sensors: challenges and opportunities for democratization of biosensing at the micro-and nanoscale. Nanophotonics. 2023;12(21):3977–4008.
[12] Thakare Y, Dharaskar S, Unnarkat A, Sonawane SS. Nanofluid-based drug delivery systems. Appl Nanofluids Chem Bio-med Process Industry. 2022;13:303–34.
[13] He JH, He CH, Qian MY, Alsolami AA. Piezoelectric Biosensor based on ultrasensitive MEMS system. Sens Actuators A Phys. 2024;376:115664.
[14] He JH, Elgazery NS, Abd-Elazem NY. Gold nanoparticles' morphology affects blood flow near a wavy biological tissue wall: an application for cancer therapy. J Appl Comput Mech. 2024;10(2):342–56.
[15] Kou SJ, He CH, Men XC, He JH. Fractal boundary layer and its basic properties. Fractals. 2022;30(9):2250172.
[16] Mei Y, Liu YQ, He JH. On the mountain-river-desert relation. Therm Sci. 2021;25(6):4817–22.
[17] Mei Y, Liu YQ, He JH. The yellow river-bed evolution a statistical proof of the mountain-river-desert conjecture. Therm Sci. 2023;27(3A):2075–79.
[18] Wang LQ, Fan J. Nanofluids research: key issues. Nanoscale Res Lett. 2010;5(8):1241–52.
[19] Qian MY, He JH. Two-scale thermal science for modern life: making the impossible possible. Therm Sci. 2022;26(3B):2409–12.
[20] He JH, Ain QT. New promises and future challenges of fractal calculus: From two-scale thermodynamics to fractal variational principle. Therm Sci. 2020;24(2A):659–81.
[21] Tuan NH, Mohammadi H, Rezapour S. A mathematical model for COVID-19 transmission by using the Caputo fractional derivative. Chaos Soliton Fract. 2020;140:110107.
[22] Baleanu D, Mohammadi H, Shahram S. The existence of solutions for a nonlinear mixed problem of singular fractional differential equations. Adv Differ Equ. 2013;1:359.
[23] Baleanu D, Aydogn SM, Mohammadi H, Rezapour S. On modelling of epidemic childhood diseases with the Caputo-Fabrizio derivative by using the Laplace Adomian decomposition method. Alex Eng J. 2020;59(5):3029–39.
[24] Baleanu D, Jajarmi A, Mohammadi H, Rezapour S. A new study on the mathematical modelling of human liver with Caputo-Fabrizio fractional derivative. Chaos Soliton Fract. 2020;134:109705.
[25] Jumarie G. Modified Riemann–Liouville derivative and fractional Taylor series of nondifferentiable functions further results. Comput Math Appl. 2006;51(9-10):1367–76.
[26] Correa-Escudero IL, Gómez-Aguilar JF, López-López MG, Alvarado-Martínez VM, Baleanu D. Correcting dimensional mismatch in fractional models with power, exponential and proportional kernel: Application to electrical systems. Results Phys. 2022;4:105867.
[27] Zhang Y, Sun HG, Stowell HH, Zayernouri M, Hansen SE. A review of applications of fractional calculus in Earth system dynamics. Chaos Soliton Fract. 2017;102(1):29–46.
[28] Kaur L, Adel W, Inc M, Rezazadeh H, Akinyemi L. Gaussian solitary wave solutions for nonlinear perturbed Schrödinger equations with applications in nanofibers. Int J Mod Phys B. 2024;38(24):2450318.
[29] Zaman UHM, Arefin MA, Akbar MA, Uddin MH. Solitary wave solution to the space-time fractional modified Equal Width equation in plasma and optical fiber systems. Results Phys. 2023;52:106903.
[30] Zeng HJ, Wang YX, Xiao M, Wang Y. Fractional solitons: New phenomena and exact solutions. Front Phys. 2023;11:1177335.
[31] Montazeri S, Nazari F, Rezazadeh H. Solitary and periodic wave solutions of the unstable nonlinear Schrödinger as equation. Optik. 2024;297:171573.
[32] Rezazadeh H. New solitons solutions of the complex Ginzburg-Landau equation with Kerr law nonlinearity. Optik. 2018;167:218–27.
[33] Lv GJ, Tian D, Xiao M, He CH, He JH. Shock-like waves with finite amplitudes. J Appl Mech. 2024;55(1):1–7.
[34] Zaman UHM, Arefin MA, Akbar MA, Uddin MH. Analyzing numerous travelling wave behavior to the fractional-order nonlinear Phi-4 and Allen-Cahn equations throughout a novel technique. Results Phys. 2022;37:105486.
[35] Akram G, Sadaf M, Zainab I. Observations of fractional effects of β-derivative and M-truncated derivative for space time fractional Phi-4 equation via two analytical techniques. Chaos Soliton Fract. 2022;154:111645.
[36] Rezazadeh H, Tariq H, Eslami M, Mirzazadeh M, Zhou Q. New exact solutions of nonlinear conformable time-fractional Phi-4 equation. Chinese J Phys. 2018;56(6):2805–16.
[37] Körpinar Z. Some analytical solutions by mapping methods for non-linear conformable time-fractional PHI-4 equation. Therm Sci. 2019;23(S6):S1815–22.
[38] Khater MMA. De Broglie waves and nuclear element interaction; Abundant waves structures of the nonlinear fractional Phi-four equation. Chaos Soliton Fract. 2022;163:112549.
[39] Chen HY, Zhu QH, Qi JM. Further results about the exact solutions of conformable space-time fractional Boussinesq equation (FBE) and breaking soliton (Calogero) equation. Results Phys. 2022;37:105428.
[40] Peregrine DH. Long waves on a beach. J Fluid Mech. 1967;27(4):815–27.
[41] Hosseini K, Ansari R. New exact solutions of nonlinear conformable time-fractional Boussinesq equations using the modified Kudryashov method. Wave Random Complex. 2017;27(4):628–36.
[42] Çerdik-Yaslan H, Girgin A. SITEM for the conformable space-time fractional Boussinesq and (2.1)-dimensional breaking soliton equations. J Ocean Eng Sci. 2020;6(3):228–36.
[43] Nisar KS, Akinyemi L, Inc M, Şenol M, Mirzazadeh M, Houwe A, et al. New perturbed conformable Boussinesq-like equation: soliton and other solutions. Results Phys. 2022;33:105200.
[44] Jumarie G. Fractional partial differential equations and modified Riemann–Liouville derivative new methods for solution. J Appl Math Comput. 2007;24(1–2):31–48.
[45] He JH, Elagan SK, Li ZB. Geometrical explanation of the fractional complex transform and derivative chain rule for fractional calculus. Phys Lett A. 2012;376(4):257–9.
[46] Li ZB, He JH. Fractional complex transform for fractional differential equations. Math Comput Appl. 2010;15(5):970–3.
[47] Ain QT, He JH, Anjum N, Ali M. The fractional complex transform: a novel approach to the time-fractional Schrodinger equation. Fractals. 2020;28(7):2050141.
[48] Han C, Wang YL, Li ZY. A high-precision numerical approach to solving space fractional Gray-Scott model. Appl Math Lett. 2022;125:107759.

[49] He CH, Liu C. Fractal dimensions of a porous concrete and its effect on the concreteas strength. Facta Univ-Ser Mech. 2023;21(1):137–50.
[50] Gao XL, Zhang HL, Wang YL, Li ZY. Research on pattern dynamics behavior of a fractional vegetation-water model in arid flat environment. Fractal Fract. 2024;8(5):264.
[51] Gao XL, Li ZY, Wang YL. Chaotic dynamic behavior of a fractional-order financial system with constant inelastic demand. Int J Bifurcat Chaos. 2024;34(9):2450111.
[52] Tian D, Ain QT, Anjum N, He CH, Cheng B. Fractal N/MEMS: from pull-in instability to pull-in stability. Fractals. 2021;29(2):2150030.
[53] He JH, Yang Q, He CH, Alsolami AA. Pull-down instability of the quadratic nonlinear oscillators. Facta Univ-Ser Mech. 2023;21(2):191–200.
[54] Li XJ, Wang D, Saeed T. Multi-scale numerical approach to the polymer filling process in the weld line region. Facta Univ-Ser Mech. 2022;20(2):363–80.